

Precision measurements of the ionization energy of the ground state and the wavelengths of the $nl-2l'$ ($n=4-15$) spectral lines of the Ne-like ion Ni XIX

A. I. Magunov, V. M. Dyakin, T. A. Pikuz, I. Yu. Skobelev, and A. Ya. Faenov

*All-Russian Scientific Research Institute of Physicotechnical and Radio-Engineering Measurements,
141570 Mendeleevo, Moscow Region, Russia*

A. Osterheld and V. Goldstein

Lawrence Livermore National Laboratory, Livermore, California 94550 USA

F. Flora, P. DiLazzaro, S. Bollanti, N. Lizi, and T. Letardi

ENEA, Frascati, Italy 00044

A. Reale and P. Palladino

Aquila University, Aquila, Italy

D. Batani and A. Mauri

Milan University, Milan, Italy

A. Skafati and L. Reale

Physics Laboratory of the Sanitation Institute, Rome, Italy

(Submitted January 10, 1996)

Zh. Éksp. Teor. Fiz. **110**, 499–509 (August 1996)

The spectral lines of the Ne-like ion Ni XIX, corresponding to $nl-2l'$ transitions with $n=4-15$, have been recorded for the first time in the emission spectra of a laser plasma. The wavelengths of the indicated transitions have been measured with an accuracy of $\pm(0.5-2.5)$ mÅ, using the spectral lines of the H- and He-like ions of Na, Mg, and Cl as references.

The ionization potential of Ne-like Ni XIX has been measured. The strong interaction of the $2s^2 2p^5 5d$ and $2s 2p^6 4p$ configurations of this ion has been experimentally confirmed.

© 1996 American Institute of Physics.[S1063-7761(96)01108-0]

1. INTRODUCTION

The study of the resonant series of multicharged ions is extremely crucial for a number of reasons. First, this is a traditional problem of experimental atomic spectroscopy (the identification of spectral lines and the measurement of their wavelengths) and makes it possible to judge the quality of various methods of purely theoretical calculation of the atomic structures. Second, this is important for developing spectroscopic methods for diagnosing high-temperature plasma. Finally, such a study presents one of the few possibilities of measuring the ionization potentials of multicharged ions.

Experimental studies of resonance series of multicharged ions with a simple structure (H-, He-, Li-, and Ne-like ions) are usually not especially difficult for the first terms of the series, with $\Delta n = n - n_g = 1, 2, 3$ (n and n_g are the principal quantum numbers of the optical electron in the excited and ground states), but become much more complicated for $\Delta n \gg 1$, since the line intensities usually decrease rather quickly with increasing Δn . For example, in the case of Ne-like ions with nuclear charges $Z_{\text{nucl}} \geq 26$, until recently, as a rule, only resonant series with $\Delta n \leq 5$ could be studied (see the review in Ref. 1), and only very recently have the lines of Ne-like Mo XXXIII with $\Delta n \leq 16$ been studied in the plasma of the Alcator C-Mod tokamak.²

The appearance of extremely fast, focusing x-ray spectrographs with spherically curved crystals^{3,4} makes it possible to record the higher terms of the resonant series of multicharged ions by means of plasma sources that are more accessible for spectroscopists, such as a laser plasma. We showed in our earlier paper⁵ that, for example, when laser pulses with very moderate values of the energy parameters were used ($E_{\text{las}} \leq 10$ J, $\tau_{\text{las}} \approx 1$ ns), it was possible to study transitions with $\Delta n \approx 10$ in He-like Al XII. In the work reported here, using about the same energetics of the plasma sources, we have succeeded for the first time in studying the resonant series of the Ne-like ion Ni XIX for $\Delta n \leq 13$.

2. EXPERIMENTAL SETUP

The experiments were carried out using two different laser systems.

In the first case, a Nd laser with a pulse energy of up to 10 J and a pulsewidth of 2 ns was used to create the plasma.⁶

In the second case, the plasma was created by the radiation of an XeCl excimer laser with an active volume of $9 \times 4 \times 100$ cm³ and a wavelength of $\lambda = 0.308$ μm.⁷ The pulse energy was 2 J with a pulsewidth of 12 ns. The laser operated with a repetition frequency of 10 Hz. Its radiation was focused on the surface of a solid target into a spot ≈ 70 μm in diameter, so that the flux density of the heating

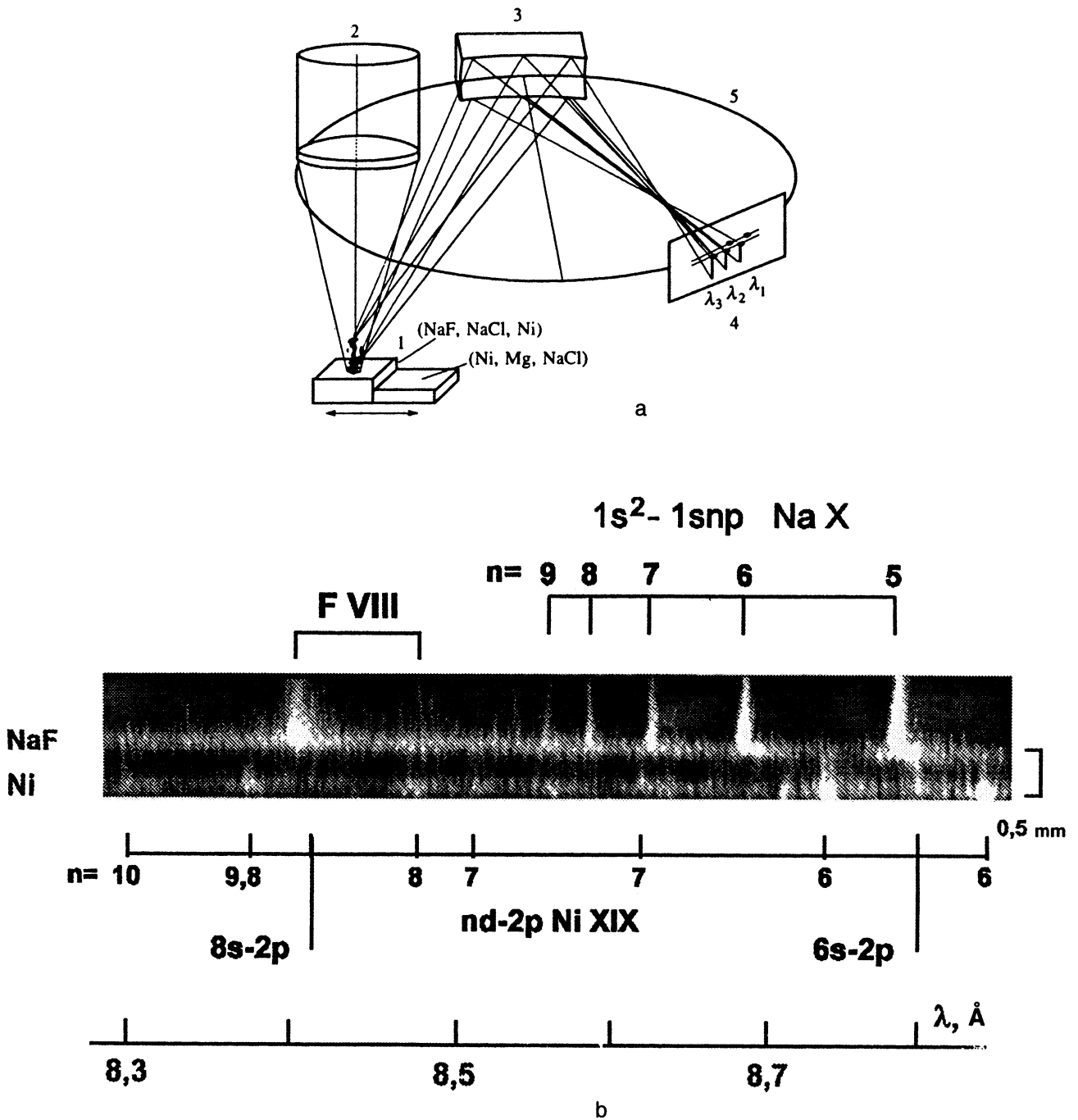


FIG. 1. (a) Experimental layout: 1—stepped target, 2—laser beam, 3—spherically curved crystal, 4—photographic plate, 5—Rowland circle. (b) Example of a luminescence spectrogram of the plasma created by the XeCl laser radiation.

radiation in this case was $\approx 4 \times 10^{12} \text{ W/cm}^2$, while in the first case the flux density was higher ($\approx 3 \times 10^{13} - 10^{14} \text{ W/cm}^2$).

In both cases, a stepped target was used (see Fig. 1), where one part contained the material being studied (nickel) and the other part contained a material whose spectral lines were used as a reference (NaCl, NaF, Mg).

The x radiation of the plasma in both cases was recorded by two spectrographs with spherically curved mica crystals, the radii of their spherical surfaces being 100 mm and 186 mm. The crystals, the plasma, and the photographic plate (see Fig. 1) were arranged in accordance with the FSPR-1M

system,⁴ in which the spectra are simultaneously recorded with high spectral resolution ($\lambda/\Delta\lambda \geq 5000$) and a spatial resolution of $\approx 20 \mu\text{m}$ along the expansion direction of the laser plasma. Since the field of view of the spectrographs was $\approx 0.3 - 0.7 \text{ \AA}$, while the extent of the spectrum being studied was larger ($\approx 1.3 \text{ \AA}$), the entire range being studied, $8.0 - 9.3 \text{ \AA}$, was broken up into four overlapping sections, each of which, besides the spectral lines of the Ne-like Ni XIX, contained a sufficient number of reference lines, which chiefly consisted of the resonant series of the H- and He-like Na ions and the resonant and intercombination lines of the

TABLE I. Spectral lines used to calibrate the spectrum of Ni XIX (n is the order of reflection of the crystal).

Transition	Ion	n	λ , Å
$5p \ ^2P_{1/2,3/2} - 1s \ ^2S_{1/2}$	Na XI	2	7.8332
$4p \ ^2P_{1/2,3/2} - 1s \ ^2S_{1/2}$	Na XI	2	8.0211
$3p \ ^2P_{1/2,3/2} - 1s \ ^2S_{1/2}$	Na XI	2	8.4595
$7 \ ^1P_1 - 1 \ ^1S_0$	Na X	2	8.6258
$6 \ ^1P_1 - 1 \ ^1S_0$	Na X	2	8.6863
$5 \ ^1P_1 - 1 \ ^1S_0$	Na X	2	8.7884
$2 \ ^1P_1 - 1 \ ^1S_0$	Cl XVI	4	4.4443
$2 \ ^3P_1 - 1 \ ^1S_0$	Cl XVI	4	4.4679
$4 \ ^1P_1 - 1 \ ^1S_0$	Na X	2	8.9827
$4C$	Cu XX	2	9.1055
$2 \ ^1P_1 - 1 \ ^1S_0$	Mg XI	2	9.1681
$2 \ ^3P_1 - 1 \ ^1S_0$	Mg XI	2	9.2307
j satellite	Mg X	2	9.3206

He-like ions Mg XI and Cl XVI, with well-known wavelengths (see Table I). Examples of the resulting spectrograms are shown in Figs. 1–3.

For the first subrange 7.8–8.5 Å (Fig. 4), the reference lines were the Lyman lines of the H-like ion Na XI, L_β , L_γ , and L_δ (see Table I). The range from 8.5 to 8.8 Å was covered by the L_β lines of Na XI and the lines of the resonance series $n^1P_1 - 1^1S_0$ of the He-like ion Na X with $n=5, 6, 7$ (Fig. 5). The third range, from 8.8 to 9.0 Å, between the $5^1P_1 - 1^1S_0$ and $4^1P_1 - 1^1S_0$ lines of Na X in second order, is covered by the resonant and intercombination lines of the He-like ion Cl XVI from the fourth order of reflection (see Fig. 6). Finally, the longest-wavelength section of the spectrum, from 9.1 to 9.3 Å, obtained in a laser plasma created by the radiation of a XeCl laser (Fig. 7), contains the resonant and intercombination lines of the He-like ion Mg XI and the well-known dielectronic j satellite of

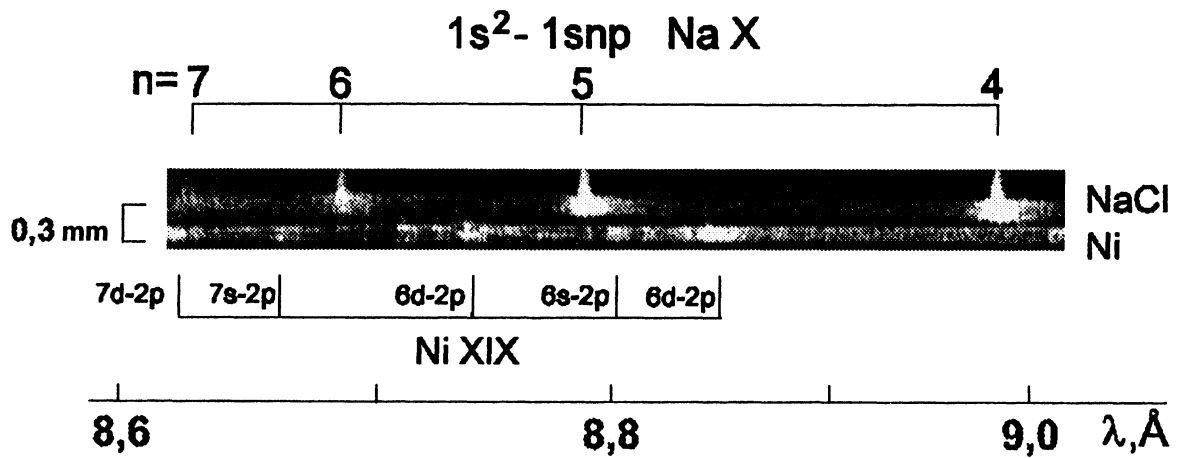


FIG. 2. Luminescence spectrogram of the laser plasma in the region $\lambda = 8.6\text{--}9.0$ Å. The plasma was created by a Nd laser.

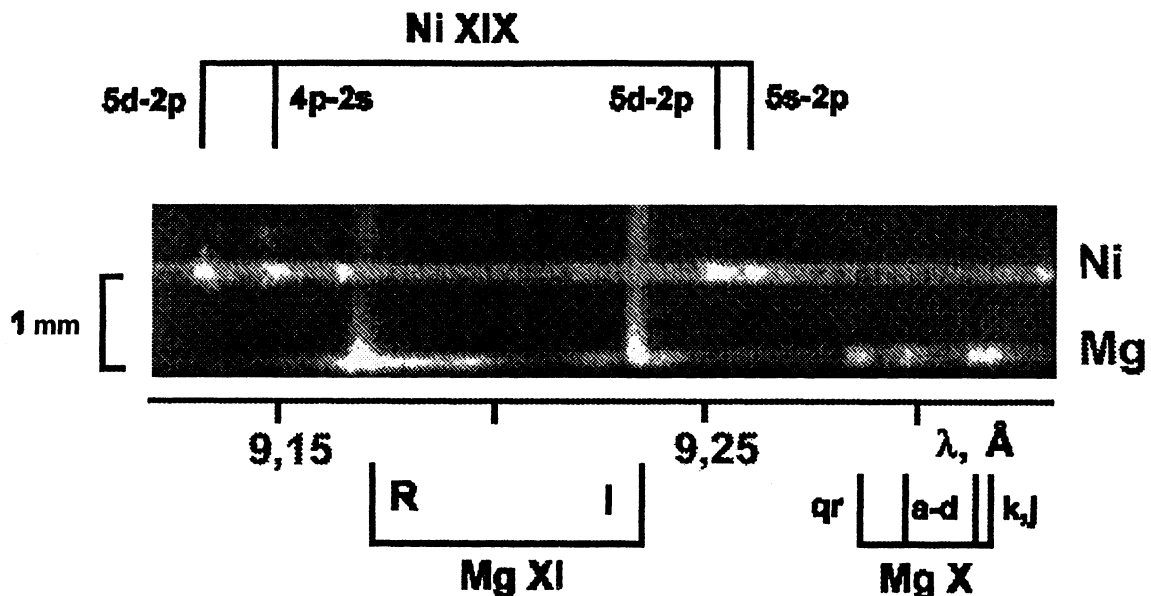


FIG. 3. Example of a luminescence spectrogram of plasma heated by a XeCl excimer laser.

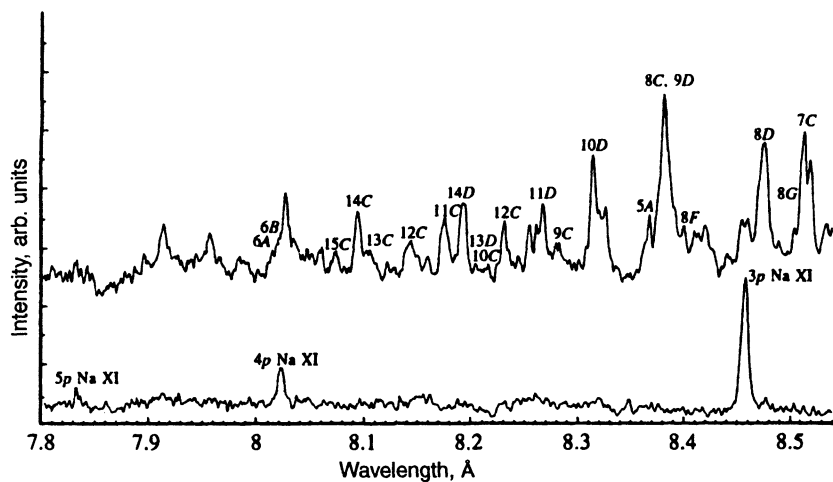


FIG. 4. Densitometer tracings of the emission spectra of a plasma of Ni + Na (above) and of NaF (below) for the 7.8–8.5 Å region. The plasma was created by a Nd laser.

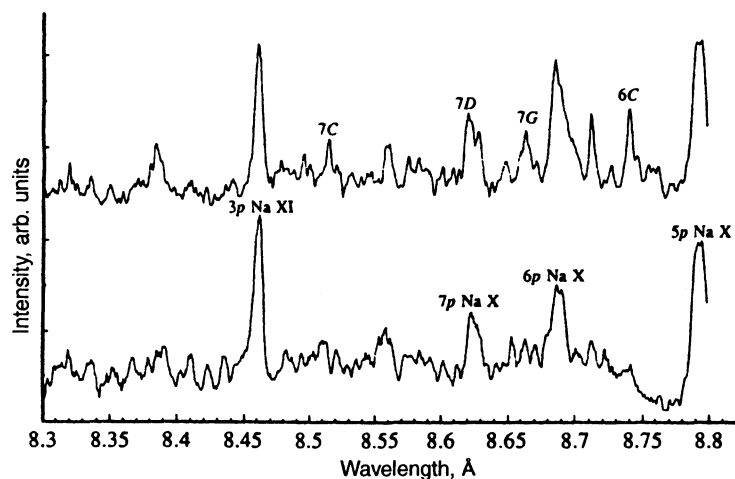


FIG. 5. Densitometer tracings of the emission spectra of a plasma of Ni + Na (above) and of NaF (below) for the 8.3–8.8 Å region. The plasma was created by a Nd laser.

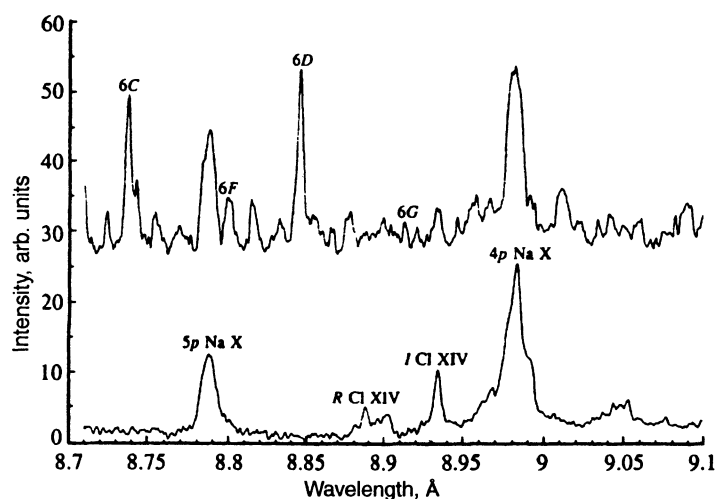


FIG. 6. Densitometer tracings of the emission spectra of a plasma of Ni + NaCl (above) and of NaCl (below) for the 8.7–9.1 Å region. The plasma was created by a Nd laser.

Mg x. The 4C line of the Ne-like ion Cu xx was also used as a secondary reference (see Table I). Using these lines made it possible to determine the dispersion dependence for each range with an accuracy no worse than 0.5–1.0 mÅ, which corresponds to the laser-plasma parameters that determine the widths of the spectral lines that limit the spectral resolution.

3. RESULTS AND DISCUSSION

To identify the lines of Ne-like Ni XIX, whose wavelengths were determined from the experimental spectra, the

Ni XIX energy levels were calculated theoretically, taking into account interconfiguration interaction and relativistic corrections, using the software package RELAC.^{8–10} The shortest-wavelength section of the spectrum, shown in Fig. 4, has the most complex line structure. Superposition of the lines of not only Ne-like but also F- and O-like ions is characteristic of this section of the spectrum, which makes it much more complicated to identify the lines with high n located in this range. Taking into account the results of the theoretical calculation of the wavelengths and transition

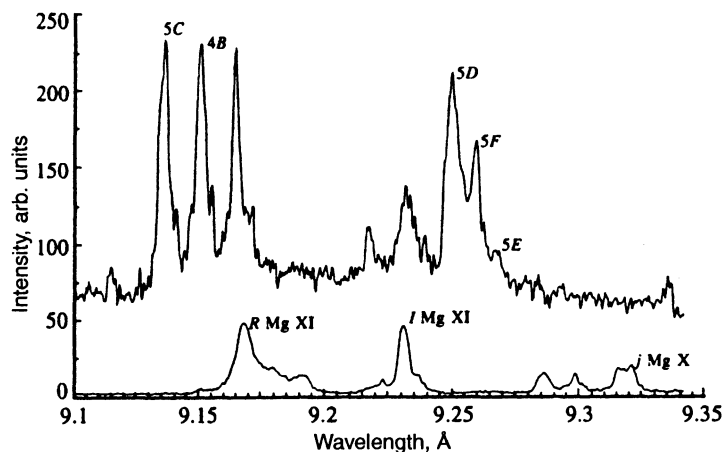


FIG. 7. Densitometer tracings of the emission spectra of a plasma of Ni + Mg (above) and of Mg (below) for the 9.1–9.35 Å region. The plasma was created by a XeCl laser.

probabilities and the complications mentioned above, it is possible to identify the lines indicated in Fig. 4. These are mainly the lines of the most intense series, nC and nD . It is possible to indicate single lines of other series, $5A$, $6A$, $6B$, $8G$, and $8F$ (see Table II for the notation for the transitions). The highest observed terms of the series correspond to the $15C$ and $14D$ transitions. The anomalously high intensities of the $14C$ and $11C$ lines are apparently associated with superposition of the lines of ions of different multiplicity. The same is true for the $11D$ line. The $8C$ and $9D$ lines are not resolved in the experiment.

The next section of the spectrum, shown in Fig. 5, contains the well-isolated lines $6C$, $7C$, $7G$, and $7D$. The difference of the measured wavelengths for these lines from the results of calculation is less than ± 1.4 mÅ. Besides these lines, other intense lines are observed that belong to ions of another multiplicity.

Figure 6 shows a spectrum on which the $6G$, $6D$, and $6F$ lines are identified. The difference from the calculated results is also less than 1.2 mÅ in this case. Finally, the longest-wavelength section is shown in Fig. 7. Of the lines identified in this figure, the greatest difference from the calculated wavelength occurs for the $4B$ line. A comparison of the line intensity and the transition probabilities suggests that this difference is also associated with overlap of the lines.

The results of the wavelength measurements of the identified spectral lines of the Ni XIX ion are shown in Table III,

TABLE II. Designations of the transitions of various series in the Ne-like ion.

Transition		
jj coupling	LS coupling	Designation
$(2\bar{s}_{1/2}n\bar{p}_{3/2})_1 - 2s^2$	$^1P_1 - ^1S_0$	nA
$(2\bar{s}_{1/2}n\bar{p}_{1/2})_1 - 2s^2$	$^3P_1 - ^1S_0$	nB
$(2\bar{p}_{1/2}n\bar{d}_{3/2})_1 - 2s^2$	$^1P_1 - ^1S_0$	nC
$(2\bar{p}_{3/2}n\bar{d}_{5/2})_1 - 2s^2$	$^3D_1 - ^1S_0$	nD
$(2\bar{p}_{3/2}n\bar{d}_{3/2})_1 - 2s^2$	$^3P_1 - ^1S_0$	nE
$(2\bar{p}_{1/2}n\bar{s}_{1/2})_1 - 2s^2$	$^1P_1 - ^1S_0$	nF
$(2\bar{p}_{3/2}n\bar{s}_{1/2})_1 - 2s^2$	$^3P_1 - ^1S_0$	nG

Note. An overline in the designation of a configuration corresponds to a vacancy in the subshell.

along with the results of the theoretical calculation of the wavelengths and radiative transition probabilities and the experimental data obtained earlier in Refs. 11 and 12.

An analysis of the dependence of the calculated $nd-2p$ radiative transition probabilities A_{nd-2p} on n shows that there are nonmonotonic sections on these dependences, associated with strong interaction of the $2s^22p^5nd$, $2s^22p^5n'd$, and $2s2p^6n''l$ configurations for certain n , n' , and n'' values. This shows up especially clearly on the n dependence of the oscillator strengths f_{2p-nd} of these transitions, or, more precisely, the n^3f_{2p-nd} values [where the factor n^3 eliminates the main part of the $f(n)$ dependence], which are shown in Fig. 8 for the $nC(2p_{1/2}-nd_{3/2})$ and $nD(2p_{3/2}-nd_{5/2})$ series. It can be seen from this figure that, as a result of the interaction of the $2s^22p^55d$ and $2s^22p^64p$ states with total momentum $J=1$, the transition probability $A_{5d_{3/2}-2p_{1/2}}$ (line $5C$) is anomalously large, while the interaction of the $2s^22p^58d$, $2s^22p^59d$, and $2s2p^55p$ states with $J=1$ increases the probability $A_{8d_{3/2}-2p_{1/2}}$ (line $8C$) and decreases $A_{9d_{5/2}-2p_{3/2}}$ (line $9D$).

Since lines $8C$ and $9D$ are not resolved in the experimental spectrum, it is simplest experimentally to check the presence of this strong configuration interaction from the $5C$ line. To do this, we consider the intensity ratio $\alpha = I_{5C}/I_{5D}$ of lines $5C$ and $5D$. For a plasma density of $N_e \approx 10^{21}$ cm $^{-3}$, characteristic of the conditions of the experiments of this paper, the populations of the states with the same principal quantum number $n \geq 5$ are proportional to their statistical weights and consequently the ratio is $\alpha = I_{5C}/I_{5D} = A_{5d_{3/2}-2p_{1/2}}/A_{5d_{5/2}-2p_{3/2}}$. Neglecting configuration mixing, this ratio should amount to $\alpha_{nm} = 0.65$, and taking it into account, $\alpha_m = 1.095$; i.e., if configuration interaction were absent, the $5C$ line would be less intense than the $5D$ line by a factor of almost two. As can be seen from Fig. 7, this is not so, and the experimental value of I_{5C}/I_{5D} is $\alpha_{exp} = 1.09$, which corresponds to the result of a calculation taking into account configuration mixing.

The results shown in Table III can be used to determine the ionization potential of the Ni XIX ion. To do this, by analogy with Refs. 13 and 10, it is possible to use the quantum-defect method and approximate the resulting ener-

TABLE III. Spectral lines of the Ni XIX ion, identified in the emission spectra of a laser plasma.

Line	Transition	$\lambda_{\text{exp}}, \text{\AA}$	$\lambda_{\text{theor}}, \text{\AA}$	$\lambda_{\text{exp}} - \lambda_{\text{theor}}$	$A_{\text{rad}}, \text{sec}^{-1}$	$\lambda_{\text{exp}}, \text{\AA}$ [11]	$\lambda_{\text{exp}}, \text{\AA}$ [Ref.12]
6A	2s - 6p	8.0136(10)	8.0122	0.0014	$8.217 \cdot 10^{11}$	-	-
6B	2s - 6p	8.0162(10)	8.0153	0.0009	$1.662 \cdot 10^{11}$	-	-
15C	2p - 15d	8.0737(8)	8.0729	0.0008	$1.220 \cdot 10^{11}$	-	-
14C	2p - 14d	8.0930(25)	8.0901	0.0029	$1.478 \cdot 10^{11}$	-	-
13C	2p - 13d	8.1117(10)	8.1115	0.0002	$1.853 \cdot 10^{11}$	-	-
12C	2p - 12d	8.1391(10)	8.1387	0.0004	$2.421 \cdot 10^{11}$	-	-
11C	2p - 11d	8.1753(15)	8.1739	0.0014	$2.972 \cdot 10^{11}$	-	-
14D	2p - 14d	8.1853(25)	8.1850	0.0003	$2.685 \cdot 10^{11}$	-	-
13D	2p - 13d	8.2048(20)	8.2068	-0.0020	$3.703 \cdot 10^{11}$	-	-
10C	2p - 10d	8.2172(25)	8.2208	-0.0036	$3.923 \cdot 10^{11}$	-	-
12D	2p - 12d	8.2354(10)	8.2347	0.0008	$4.007 \cdot 10^{11}$	-	-
11D	2p - 11d	8.2686(15)	8.2705	-0.0019	$5.997 \cdot 10^{11}$	-	-
9C	2p - 9d	8.2835(10)	8.2852	-0.0017	$4.670 \cdot 10^{11}$	-	-
10D	2p - 10d	8.3196(10)	8.3184	0.0012	$6.860 \cdot 10^{11}$	-	-
5A	2s - 5p	8.3677(5)	8.3676	0.0001	$1.194 \cdot 10^{12}$	-	-
5B	2s - 5p		8.3731		$9.887 \cdot 10^{10}$	-	-
8C	2s - 8d	8.3815(25)	8.3768	0.0047	$1.340 \cdot 10^{12}$	-	-
9D	2p - 9d	8.3815(25)	8.3842	-0.0027	$6.790 \cdot 10^{11}$	-	-
8F	2p - 8s	8.4002(7)	8.4007	-0.0005	$5.377 \cdot 10^{10}$	-	-
8D	2p - 8d	8.4767(7)	8.4774	-0.0007	$1.486 \cdot 10^{12}$	-	-
7C	2p - 7d	8.5136(8)	8.5151	-0.0014	$9.633 \cdot 10^{11}$	8.5120	-
7D	2p - 7d	8.6193(8)	8.6180	0.0013	$2.011 \cdot 10^{12}$	8.6140	-
7G	2p - 7s	8.6579(8)	8.6580	-0.0001	$4.723 \cdot 10^{10}$	-	-
6C	2p - 6d	8.7381(8)	8.7372	0.0009	$1.673 \cdot 10^{12}$	8.7310	8.7440
6F	2p - 6s	8.7996(8)	8.8002	-0.0005	$1.680 \cdot 10^{10}$	-	-
6D	2p - 6d	8.8456(8)	8.8444	0.0012	$2.954 \cdot 10^{12}$	8.8460	8.8490
6G	2p - 6s	8.9132(10)	8.9123	0.0009	$6.920 \cdot 10^{10}$	-	-
5C	2p - 5d	9.1354(12)	9.1339	0.0016	$4.457 \cdot 10^{12}$	9.1280	9.1390
4B	2s - 4p	9.1497(25)	9.1458	0.0039	$1.516 \cdot 10^{12}$	-	9.1530
5D	2p - 5d	9.2487(8)	9.2479	0.0009	$4.163 \cdot 10^{12}$	9.2460	9.2540
5F	2p - 5s	9.2584(5)	9.2582	0.0002	$6.780 \cdot 10^{11}$	-	-
5E	2p - 5d	9.2662(7)	9.2669	-0.0007	$8.207 \cdot 10^{10}$	-	-

gies $E_{nC(D)} \propto 1/\lambda_{nC(D)}$ of the excited levels by a formula of the type

$$E_{nC(D)} = I_{C(D)} - \frac{Z^2 \text{Ry}}{\left(n + a_{C(D)} + \frac{b_{C(D)}}{n} + \frac{c_{C(D)}}{n^2} \right)}, \quad (1)$$

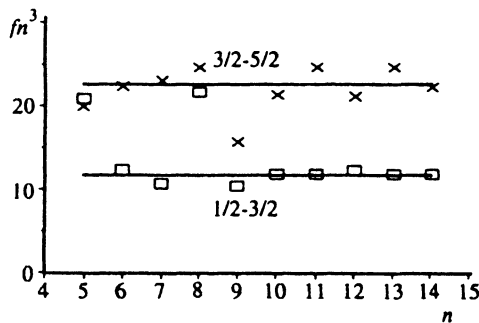


FIG. 8. Oscillator strengths f of the transitions $2p_{1/2} - nd_{3/2}$ (series nC) and $2p_{3/2} - nd_{5/2}$ (series nD) in the Ne-like ion Ni XIX. The value of $n^3 f$ is plotted along the y axis, the straight lines correspond to a calculation neglecting configuration mixing, and the points to a multiconfigurational calculation.

where parameters $a_{C(D)}$, $b_{C(D)}$, and $c_{C(D)}$ determine the value of the quantum defect. Since the nD series converges to the ground state $2s^2 2p^5 \ ^2P_{3/2}$ of the F-like ion Ni XX, I_D is the first ionization potential of the Ni XIX ion, while I_C is the total ionization potential of Ni XIX and the $2s^2 2p^5 \ ^2P_{3/2} - 2s^2 2p^5 \ ^2P_{1/2}$ transition energy of the Ni XX ion. The values of parameters I , a , b , and c were determined in this work by the method of least squares, using either the theoretical or the experimental values as energies $E_{nC(D)}$. The lines 5C, 8C, and 9D were left out of consideration, since their positions are shifted in an irregular way because of configuration interaction. The I_C and I_D values thus obtained are shown in Table IV. It can be seen from this table, first, that the $I_{C(D)}$ values obtained using the theoretical and experimental energy levels coincide to within experimental error; second, that the ionization potential $I_0 = 1540.1 \pm 0.5$

TABLE IV. Values of I_C and I_D obtained using theoretical and experimental values of the energies of the excited states of the Ni XIX ion.

I_D , eV		I_C , eV		$I_C - I_D$, eV		$E(2s^2 2p_{3/2}^5 - 2s^2 2p_{1/2}^5)$
theory	exp.	theory	exp.	theory	exp.	exp., Ref. 15
1539.96	1540.1(5)	1557.82	1557.1(8)	17.86	17.0(1.3)	17.85

eV obtained from the experimental data agrees with the earlier measured value¹⁴ of $I_0 = 1541 \pm 1$ eV but has higher precision; and, third, that the difference $I_C - I_D$ obtained in this paper coincides within the indicated limits of error with the result of a direct measurement¹⁵ of the ${}^2P_{3/2} - {}^2P_{1/2}$ magnetic-dipole transition energy in the Ni XX ion. We should point out that the ionization potential in Ref. 14 was derived from data on the wavelengths of the $2s^2 2p^5 nd^3 D_1 - 2s^2 2p^6$ ($n=3-6$) transitions measured in Refs. 16 and 17 with an error of ± 0.005 Å, which caused a larger error of the I value.

4. CONCLUSION

Thus, by using modern x-ray-spectral technology in our work, we were able, even with extremely low-power plasma sources, to detect for the first time the $nl - nl'$ transitions in Ne-like Ni XIX for $n=8-15$ and to measure their wavelengths with an accuracy of $\pm(0.5-2.5)$ mÅ. This in turn made it possible with higher precision than earlier to determine the ionization potential of the Ni XIX ion, which amounted to 1540.1 ± 0.5 eV. An analysis of the relative intensities of the observed spectral lines showed the presence of strong interaction of the $2s^2 2p^5 5d$ and $2s 2p^6 4p$ configurations.

¹V. A. Boiko, V. G. Pal'chikov, I. Yu. Skobelev, and A. Ya. Faenov, *X-ray Spectroscopy of Multicharged Ions* (Energoatomizdat, Moscow, 1988).

²J. E. Rice, K. B. Fournier, M. A. Graf *et al.*, *Phys. Rev. A* **51**, 3551 (1995).

³T. A. Pikuz, A. Ya. Faenov, S. A. Pikuz *et al.*, *J. X-ray Sci. Tech.* **5**, 323 (1995).

⁴I. Yu. Skobelev, A. Ya. Faenov, B. A. Bryunetkin *et al.*, *Zh. Eksp. Teor. Fiz.* **108**, 1263 (1995) [*JETP* **81**, 692 (1995)].

⁵V. M. Dyakin, A. Ya. Faenov, A. I. Magunov *et al.*, *Physica Scripta* **52**, 201 (1995).

⁶A. Faenov, B. Bryunetkin, V. Dyakin *et al.*, *Phys. Rev. A* **52**, 3644 (1995).

⁷F. Flora, S. Bollanti, R. A. Cotton *et al.*, in: M. C. Richardson and G. A. Kyrala (Eds.) *Applications of Laser Plasma Radiation II*, Proc. SPIE 2523 (1995).

⁸M. Klapisch, *Comput. Phys. Commun.* **2**, 239 (1971).

⁹M. Klapisch, J. L. Schwob, B. S. Frankel, and J. Oreg, *J. Opt. Soc. Am.* **61**, 148 (1977).

¹⁰A. L. Osterheld, A. I. Magunov, V. M. Dyakin *et al.*, *Phys. Rev. A* [in press] (1996).

¹¹V. A. Boiko, A. Ya. Faenov, and S. A. Pikuz, *J. Quantum Spectrosc. Radiat. Transfer* **19**, 11 (1978).

¹²H. Gordon, M. G. Hobby, and N. J. Peacock, *J. Phys. B* **13**, 1985 (1980).

¹³W. C. Martin, *Physica Scripta* **24**, 725 (1981).

¹⁴J. Sugar and C. Corliss, *J. Phys. Chem. Ref. Data* **14**, Suppl. 2 (1985).

¹⁵N. J. Peacock, M. F. Stamp, and J. D. Silver, *Physica Scripta* **8**, 10 (1984).

¹⁶M. Klapisch, A. Bar Shalom, J. Schwob *et al.*, *Phys. Lett. A* **69**, 34 (1978).

¹⁷H. Gordon, M. G. Hobby, and N. J. Peacock, *J. Phys. B* **13**, 1985 (1980).

Translated by W. J. Manthey